Hindawi Publishing Corporation
International Journal of Antennas and Propagation
Volume 2012, Article ID 917248, 6 pages
doi:10.1155/2012/917248

Research Article

CLEAN Technique to Classify and Detect Objects in Subsurface Imaging

E. Karpat

Electronics Engineering Department, Uludag University, Gorukle, Bursa, Turkey

Correspondence should be addressed to E. Karpat, esinoz@uludag.edu.tr

Received 4 October 2012; Revised 20 November 2012; Accepted 21 November 2012

Academic Editor: Dau-Chyrh Chang

An image domain CLEAN technique, for nondestructive and noncontacting subsurface imaging, is discussed. Recently introduced finite-difference time-domain- (FDTD-) based virtual tool, GrGPR, is used to create imaging scenarios and to generate synthetic scattering data through synthetic aperture (SAR) type scanning. Matlab-based imaging algorithms are used to process recorded FDTD data. The location and the geometry of the targets are obtained by image domain CLEAN technique which is extracting scattering centers from the SAR image. The effectiveness of the algorithm is tested in simulated data.

1. Introduction

Imaging and *detection* are two keywords in searching/diagnosing tumors, buried land mines, people under debris, and so forth [1–9]. The first essential step in these tasks is subsurface imaging (SSI) which is based on illuminating an area/object with a sensor (or a group of sensors) and processing forward and/or backward scattered signal. The sensor technologies as well as computer algorithms are in a quite mature stage to accomplish these tasks. The imaging information is hidden in the difference of electromagnetic (EM) parameters (e.g., permittivity) in the environment, and identification of something within this subsurface image is an extremely difficult task which necessitates the use of intelligent detection and identification methods, adaptive noise, and clutter elimination approaches. Most of imaging algorithms rely on linear procedure to comply quick imaging requirement. Inverse scattering is a widely used imaging algorithm which is based on the reconstruction of electromagnetic properties of unknown scatterers by inverting scattered field measurements [10]. Inversion procedures are usually quite complex and time consuming, especially when high-resolution images are needed. In the literature, some deterministic and stochastic approaches have been proposed for solving this problem. Stochastic approaches are global optimization methods and are usually based on population-based solutions such as genetic algorithm, ant colony optimization, and particle swarm optimization, which are optimization methods used in electromagnetics for image reconstruction [10–17]. It is still a quite difficult task to develop effective reconstruction procedures, and better algorithms are still required. Tests should be performed with data, recorded or synthetically generated under scenarios as realistic as possible.

Data acquisition within such realistic experiments is very expensive and time consuming and sometimes could be dangerous as well. Therefore, numerical models are very attractive. Numerical models have gained high importance in electromagnetics (EM). Instead of using expensive and time consuming experimental setups, numerical modeling of complex electromagnetic problems is highly preferred. There are many powerful time and frequency domain methods in EM. The most famous one is the finite-difference time-domain (FDTD) method [18]. The FDTD method is easy to understand and implement and has been widely used in subsurface numerical modeling [19, 20]. With the aid of visualization, FDTD has become very powerful in EM not only for research but also for engineering education purposes. Considering the advantages and importance of easy-to-use design steps, a set of FDTD-based virtual tools

has been introduced to the use of engineering society [21–28].

In this study, SSI is discussed in 2D simplified environments. The first part of the study is focused on synthetic data acquisition. Recently introduced, 2D FDTD-based virtual EM tool, GrGPR, is used to create various SSI scenarios and to generate synthetic scattering data through synthetic aperture (SAR) type scanning. Matlab-based algorithms are used to process recorded FDTD data in order to construct the images of the objects [28]. In addition to the prior, in this study, CLEAN technique-based feature extraction method is applied to obtain the structural frame of the objects. The CLEAN technique is based on extracting scattering centers [29–31], and in this study the images obtained via this method are referred to as *scattering centers*.

2. SSI: Image Reconstruction Algorithm

In this study, GrGPR virtual tool is used in generating synthetic data for various shaped objects. The images that will be processed with CLEAN algorithm are priorly created by MATLAB-based imaging algorithms. GrGPR is used to record raw FDTD data.

GrGPR gives us the opportunity to create and locate triangular, rectangular, and/or elliptical objects, either perfect electrical conductor (PEC) or lossy, by just selecting an object and clicking/dragging the mouse (Figure 1). A flat or irregular lossy ground with buried objects may be generated. The irregular terrain is produced automatically using cubic-spline interpolation algorithm once the user locates a number of points and fills the area between the curve and the bottom (left mouse button) or top (right mouse button) boundary [27].

N (here, N is set to 50) radiators/receivers are located in pair. Gaussian pulse excitation is selected from the other signal types (i.e., continuous wave, rectangular pulse, and linear FM). The antenna pairs are activated sequentially for SAR type scanning. Then the raw signal which contains both early- and late-time responses is recorded by GrGPR receiver.

Early-time response, which consists of the transmit signal and the signal reflected from the boundary/skin layer, is obtained by repeating the GrGPR simulations without the object under investigation. Information related to the scattering object is hidden somewhere in the late-time response and can be achieved by subtracting the early-time response accordingly.

The accumulation of late-time responses from every single cell to a pair of radiator/receiver necessitates the calculation of round-trip signal delay. Denote coordinates of each cell/pixel by (x_i, y_j), where x and y are the horizontal and vertical axes, respectively. Coordinates of the kth radiator/receiver pair are denoted by (x_t^k, y_t^k). The time necessary for a round trip from the radiator to the cell/pixel and back to the receiver can then be calculated via

$$\tau_{i,j}^k = \frac{2 * \sqrt{\left(x_i - x_t^k\right)^2 + \left(y_j - y_t^k\right)^2}}{c}, \tag{1}$$

where c is the speed of light. The corresponding pixel (*distance*) index $l_{i,j}^k$ is directly obtained from

$$l_{i,j}^k = \frac{\tau_{i,j}^k}{\Delta t}, \tag{2}$$

where Δt is the FDTD time step. The field intensity $I(i, j)$ of each cell (i.e., the image color) is then formed as

$$I(i,j) = \sum_{k=1}^{N} a_{i,j}^k \left(l_{i,j}^k\right), \tag{3}$$

where $a_{i,j}^k$ is the intensity at $l_{i,j}^k$. Note that round-trip delays calculated from (1) must be replaced by an expression which takes into account Snell's law if an object buried under the lossy ground is of interest. In summary, the three-step SSI algorithm is based on the calculation of the time delays of all round trips from all pixels to all scan points, noise/clutter elimination and signal enhancement (i.e., matched filtration), and superposing scattered field values corresponding to those delays.

Since the aim of this study is to examine the applicability of the CLEAN technique, the objects under investigation are assumed to be in free space and the elimination of surface effect is neglected; so the study is focused on improving the imaging quality.

3. CLEAN Algorithm

CLEAN algorithm is one of the challenging signal processing techniques for microwave imaging, which was originally developed for astronomy in 1974 [29] and adopted for microwave imaging applications since 1988 [30].

In the literature, CLEAN technique is applied for two types of image processing: one is to get rid of the clutters in the image to enhance the image quality and the other is used to determine the scattering centers of the image. The image quality enhancement is achieved by subtracting the residual image data from the original one. However, this study is focused on scattering centers method, and a sample scenario is given for the other latter.

The intensity of two-dimensional scattering centers $A_n(i_n, j_n)$ is subtracted one at a time from the priorly formed SAR image equation (3) using image domain CLEAN technique. The scattering centers are iteratively identified after each subtraction step and then removed from the progressive residual of the image, proceeding from the strongest to weakest stronger scattering center (4). This process allows for each scattering center to be more accurately distinctive in the absence of the prior. All scattering centers for a target are identified when the residual reaches a priorly identified threshold (I_{tr}). Lastly, these 2D scattering centers are placed in a multidimensional grid of 2D space (C) according to their spatial behavior (5). Consider

$$I_{(n)}(i_n, j_n) = I_{(n-1)}(i_n, j_n) - A_n(i_n, j_n), \tag{4}$$

$$\begin{aligned} C(k,1) &= i_n, \\ C(k,2) &= j_n. \end{aligned} \tag{5}$$

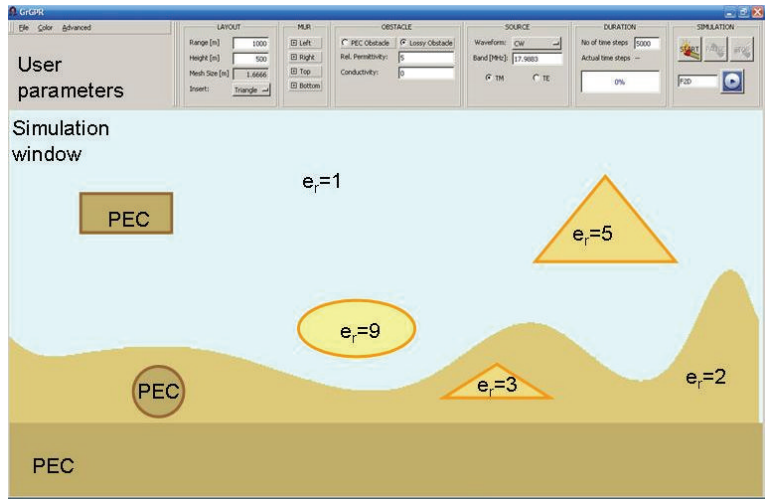

Figure 1: The front panel of the GrGPR virtual tool and user-created, either perfect electrical conductor (PEC) or lossy, triangular, rectangular, and/or elliptical objects.

It must be noted that each subtraction is performed not only for a single scattering point but within predetermined neighbourhood to increase the speed of the algorithm. The center scattering point is assumed to be the strongest one within this neighbourhood and selected as the scattering center. The flowchart of the applied image domain CLEAN algorithm is given in Figure 2.

The residual data $I_n(i_n, j_n)$ is assumed to be belonging to the clutter. When the residual data is removed from the starting image data $I_1(i_1, j_1)$, the resultant is the CLEANed image that is given in

$$I_C(i, j) = I_1(i_1, j_1) - I_{(n)}(i_n, j_n). \quad (6)$$

4. Sample Scenarios and Canonical Examples

Various SSI scenarios are created using the GrGPR tool, and scattered time data are recorded; then images are reconstructed via the SSI algorithm developed. All examples presented here are run for a Gaussian UWB pulse. The transmit/receive antenna pair is located at 50 different points around the object under investigation on a circular path and activated sequentially to perform a contour-SAR scan. All objects presented below are PEC. The images are formed by two different algorithms: SAR processing and image domain CLEAN technique which is called *scattering centers* in this study.

To prove the correctness of the applied method, a simple square PEC object is located in free space and the 50 transmit/receive antenna pairs are placed around this object (Figure 3). The original image of the object is pictured on the left. The images obtained by SAR processing and scattering center are given in the middle and on the right, respectively. The total elapsed time to reconstruct both images is 14 seconds.

In Figure 4, the examples of two PEC objects with different geometries are given. The original images of the objects (Figure 4(a)) are compared with the images obtained via SAR processing (Figure 4(b)) and scattering center (Figure 4(c)), respectively. The scattering center images are obtained for both Gauss (stars) and Linear FM-Chirp signals (diamond). The total elapsed time to reconstruct the images of each geometry is 20.4 (top) and 20.6 (bottom) seconds.

In Figure 5, a more complex object (Figure 5(a)) is preferred and the images are given for both SAR processing (Figure 5(b)) and scattering center (Figure 5(c)). The consistency of the images can be observed. The scattering corners and edges can be detected in spite of the complexity of the

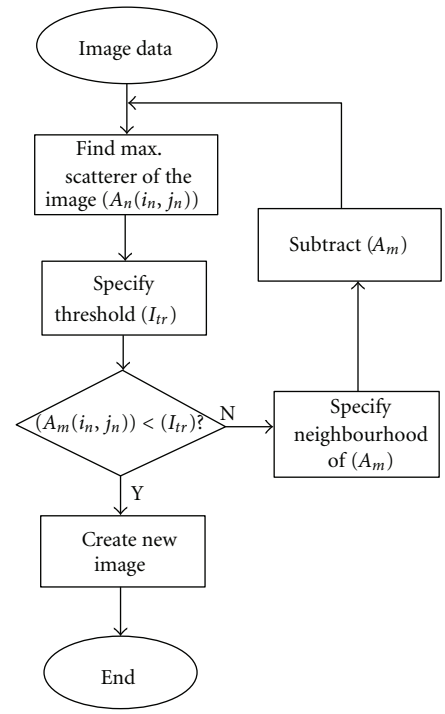

Figure 2: The flowchart of the CLEAN algorithm.

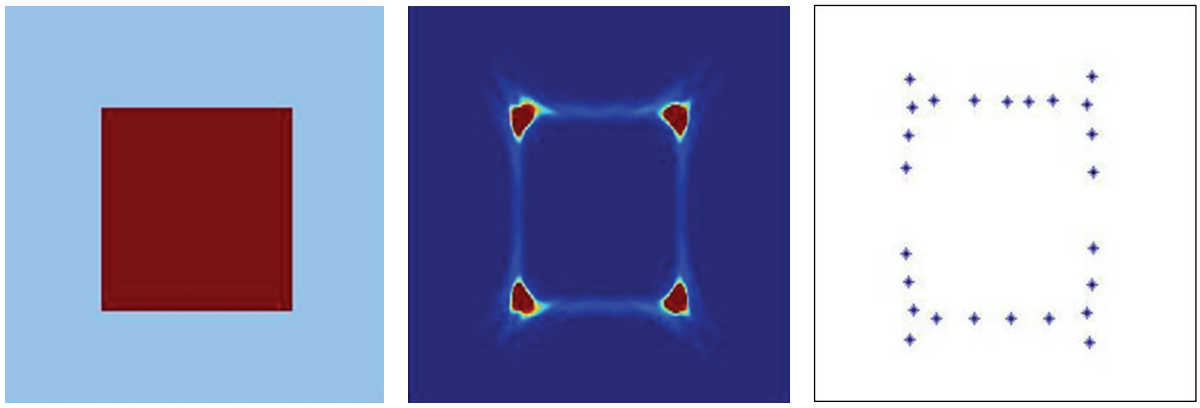

Figure 3: The original (a), SAR-processed (b), and scattering centers (c) images of a square PEC object.

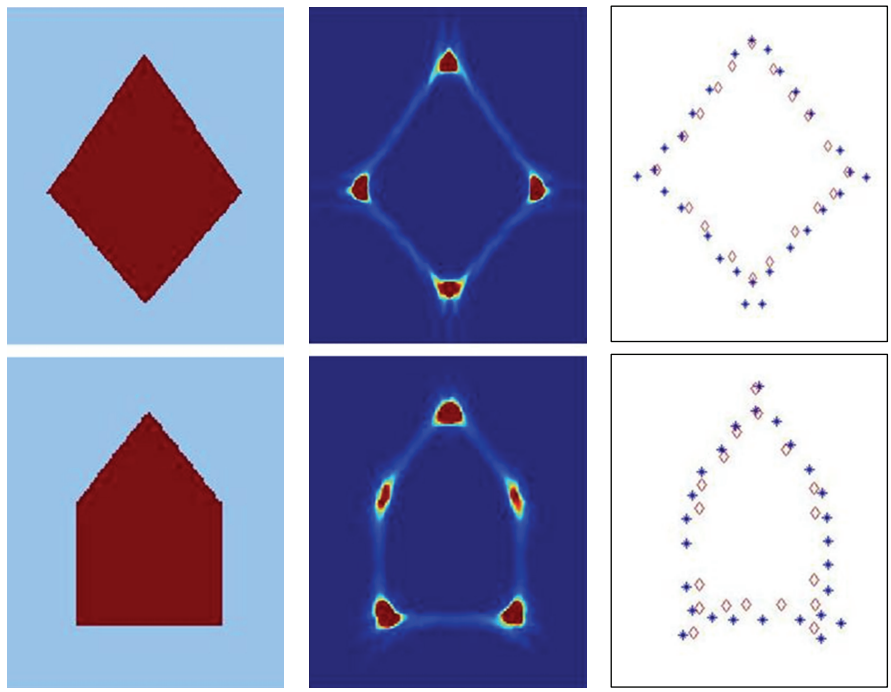

(a) (b) (c)

Figure 4: The original (a), SAR-processed (b), and scattering centers (c) images of PEC objects with two different geometries. Scattering center images are obtained for both Gauss (stars) and LFM (diamond) signals.

object. The total elapsed time to reconstruct both images is 19 seconds.

A sample for image quality enhancement is given in Figure 6. The original image is pictured in Figure 6(a). As in previous example the SAR-processed and scattering center images are obtained (Figures 6(b) and 6(c), resp.). Then the CLEANed image is reconstructed by subtracting residual image data, from the original image data, and this is pictured in Figure 6(d). It can be observed that the clutter effects due to scattering are mostly removed in the last image. The time elapsed for the SAR image, scattering centers, and the CLEANed image is 30 seconds.

5. Conclusion

A CLEAN technique-based feature extraction method, which is, in this study, referred to as *scattering center*, is discussed. A FDTD-based GrGPR virtual tool is used to generate forward scattered data synthetically. The tests are done for PEC objects with various shapes. The images, obtained with two different methods, are compared, and the consistency of the results is shown. The CLEAN technique can be used for two different approaches: image enhancement and feature extraction. The tests for image enhancement show that the clutter effects can mostly be reduced via this method. And the

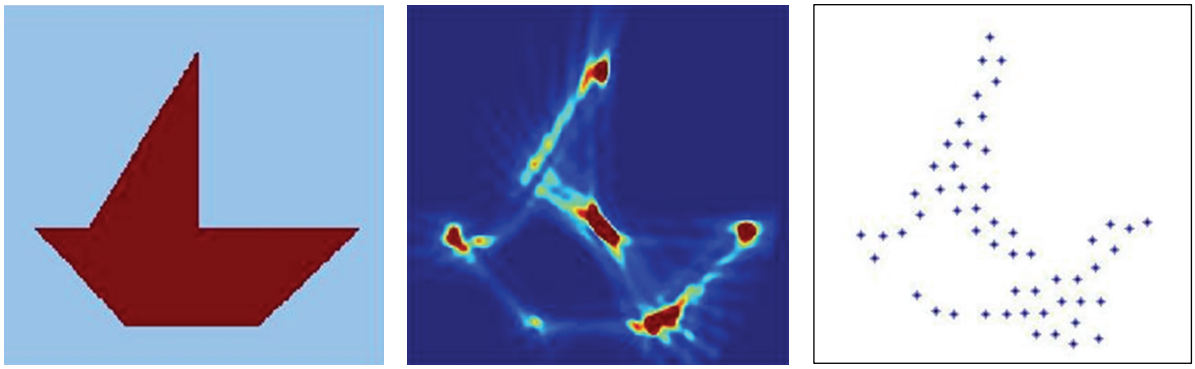

Figure 5: The original (a), SAR-processed (b), and scattering centers (c) images of a PEC object with a complex geometry.

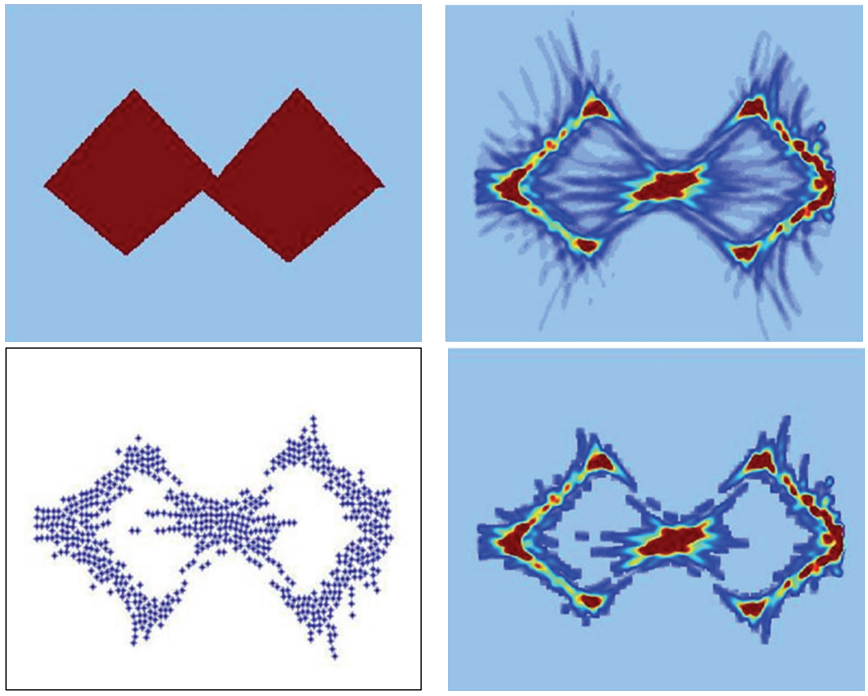

Figure 6: The original (a), SAR-processed (b), scattering centers (c), and CLEANed (d) images of a PEC object with a complex geometry.

contour of the even complex images can be obtained by the feature extraction capability of the algorithm. The CLEAN technique can be used for two different purposes, and this strengthens the method.

References

[1] X. Li, E. J. Bond, B. D. Van Veen, and S. C. Hagness, "An overview of ultra-wideband microwave imaging via space-time beamforming for early-stage breast-cancer detection," *IEEE Antennas and Propagation Magazine*, vol. 47, no. 1, pp. 19–34, 2005.

[2] X. Li and S. C. Hagness, "A confocal microwave imaging algorithm for breast cancer detection," *IEEE Microwave and Wireless Components Letters*, vol. 11, no. 3, pp. 130–132, 2001.

[3] E. C. Fear, S. C. Hagness, P. M. Meaney, M. Okoniewski, and M. A. Stuchly, "Enhancing breast tumor detection with near-field imaging," *IEEE Microwave Magazine*, vol. 3, no. 1, pp. 48–56, 2002.

[4] E. C. Fear, P. M. Meaney, and M. A. Stuchly, "Microwaves for breast cancer detection?" *IEEE Potentials*, vol. 22, no. 1, pp. 12–18, 2003.

[5] E. C. Fear, X. Li, S. C. Hagness, and M. A. Stuchly, "Confocal microwave imaging for breast cancer detection: localization of tumors in three dimensions," *IEEE Transactions on Biomedical Engineering*, vol. 49, no. 8, pp. 812–822, 2002.

[6] X. Xu, E. L. Miller, C. M. Rappaport, and G. D. Sower, "Statistical method to detect subsurface objects using array ground-penetrating radar data," *IEEE Transactions on Geoscience and Remote Sensing*, vol. 40, no. 4, pp. 963–976, 2002.

[7] Y. Wang, X. Li, Y. Sun, J. Li, and P. Stoica, "Adaptive imaging for forward-looking ground penetrating radar," *IEEE Transactions on Aerospace and Electronic Systems*, vol. 41, no. 3, pp. 922–936, 2005.

[8] T. C. Williams, E. C. Fear, and D. T. Westwick, "Tissue sensing adaptive radar for breast cancer detection-investigations of an improved skin-sensing method," *IEEE Transactions on Microwave Theory and Techniques*, vol. 54, no. 4, pp. 1308–1313, 2006.

[9] R. Banasiak and M. Soleimani, "Shape based reconstruction of experimental data in 3D electrical capacitance tomography," *NDT & E International*, vol. 43, no. 3, pp. 241–249, 2010.

[10] I. T. Rekanos, "Shape reconstruction of a perfectly conducting scatterer using differential evolution and particle swarm optimization," *IEEE Transactions on Geoscience and Remote Sensing*, vol. 46, no. 7, pp. 1967–1974, 2008.

[11] A. Randazzo, "Swarm optimization methods in microwave imaging," *International Journal of Microwave Science and Technology*, vol. 2012, Article ID 491713, 12 pages, 2012.

[12] C. H. Huang, C. C. Chiu, C. L. Li, and Y. H. Li, "Image reconstruction of the buried metallic cylinder using FDTD method and SSGA," *Progress in Electromagnetics Research*, vol. 85, pp. 195–210, 2008.

[13] C. H. Sun, C. L. Liu, K. C. Chen, C. C. Chiu, C. L. Li, and C. C. Tasi, "Electromagnetic transverse electric wave inverse scattering of a partially immersed conductor by steady-state genetic algorithm," *Electromagnetics*, vol. 28, no. 6, pp. 389–400, 2008.

[14] C. H. Sun, C. C. Chiu, W. Chien, and C. L. Li, "Application of FDTD and dynamic differential evolution for inverse scattering of a two- dimensional perfectly conducting cylinder in slab medium," *Journal of Electronic Imaging*, vol. 19, Article ID 043016, 2010.

[15] C. H. Sun, C. C. Chiu, and C. L. Li, "Time-domain inverse scattering of a two-dimensional metallic cylinder in slab medium using asynchronous particle swarm optimization," *Progress in Electromagnetics Research M*, vol. 14, pp. 85–100, 2010.

[16] C. H. Sun and C. C. Chiu, "Electromagnetic imaging of buried perfectly conducting cylinders targets using the dynamic differential evolution," *International Journal of RF and Microwave Computer-Aided Engineering*, vol. 22, no. 2, pp. 141–146, 2012.

[17] C. C. Chiu, C. H. Sun, C. L. Li, and C. H. Huang, "Comparative study of some population-based optimization algorithms on inverse scattering of a two-dimensional perfectly conducting cylinder in dielectric slab medium," *IEEE Transactions on Geoscience and Remote Sensing*, no. 99, pp. 1–19, 2012.

[18] K. S. Yee, "Numerical solution of initial boundary value problems involving Maxwell's equations in isotropic media," *IEEE Transactions on Antennas and Propagation*, vol. 14, no. 3, pp. 302–307, 1966.

[19] F. L. Teixeira, W. C. Chew, M. Straka, M. L. Oristaglio, and T. Wang, "Finite-difference time-domain simulation of ground penetrating radar on dispersive, inhomogeneous, and conductive soils," *IEEE Transactions on Geoscience and Remote Sensing*, vol. 36, no. 6, pp. 1928–1937, 1998.

[20] J. M. Bourgeois and G. S. Smith, "A complete electromagnetic simulation of the separated-aperture sensor for detecting buried land mines," *IEEE Transactions on Antennas and Propagation*, vol. 46, no. 10, pp. 1419–1426, 1998.

[21] L. Gürel and U. Oğuz, "Three-dimensional FDTD modeling of a ground-penetrating radar," *IEEE Transactions on Geoscience and Remote Sensing*, vol. 38, no. 4, pp. 1513–1521, 2000.

[22] L. Sevgi, "Modeling and simulation concepts in engineering education: virtual tools," *ELEKTRIK*, vol. 14, no. 1, pp. 113–127, 2006.

[23] G. Çakır, M. Çakır, and L. Sevgi, "A novel virtual FDTD-based microstrip circuit design and analysis tool," *IEEE Antennas and Propagation Magazine*, vol. 48, no. 6, pp. 161–173, 2006.

[24] L. Sevgi and Ç. Uluışık, "A MATLAB-based transmission-line virtual tool: finite-difference time-domain reflectometer," *IEEE Antennas and Propagation Magazine*, vol. 48, no. 1, pp. 141–145, 2006.

[25] G. Çakır, M. Çakır, and L. Sevgi, "A multipurpose FDTD-based two dimensional electromagnetic virtual tool," *IEEE Antennas and Propagation Magazine*, vol. 48, no. 4, pp. 142–151, 2006.

[26] M. Çakır, G. Çakır, and L. Sevgi, "A two-dimensional FDTD-based virtual metamaterial—wave interaction visualization tool," *IEEE Antennas and Propagation Magazine*, vol. 50, no. 3, pp. 166–175, 2008.

[27] G. Çakır, M. Çakır, and L. Sevgi, "Radar cross section (RCS) modeling and simulation—part 2: a novel FDTD-based RCS prediction virtual tool for the resonance regime," *IEEE Antennas and Propagation Magazine*, vol. 50, no. 2, pp. 81–94, 2008.

[28] E. Karpat, M. Çakır, and L. Sevgi, "Subsurface imaging, FDTD-based simulations and alternative scan/processing approaches," *Microwave and Optical Technology Letters*, vol. 51, no. 4, pp. 1070–1075, 2009.

[29] J. A. Högbom, "Aperture synthesis with a nonregular distribution of interferometric baselines," *Astronomy and Astrophysics Supplements*, vol. 15, pp. 417–426, 1974.

[30] J. Tsao and B. D. Steinberg, "Reduction of sidelobe and speckle artifacts in microwave imaging: the CLEAN technique," *IEEE Transactions on Antennas and Propagation*, vol. 36, no. 4, pp. 543–557, 1988.

[31] A. Marie Raynal, *Feature-based exploitation of multidimensional radar signatures [Dissertation]*, The University of Texas at Austin, August 2008.